Int. J. Adv. Res. Sci. Technol. Volume 12, Issue 7, 2023, pp.1036-1049

IJARST

International Journal of Advanced Research in Science and Technology

journal homepage: www.ijarst.com

ISSN 2319 – 1783 (Print)
ISSN 2320 – 1126 (Online)

Synthesis, Crystal structure, DFT investigation and Antimicrobial, Molecular docking studies of (E)-3-methoxy-N'-(1-phenylethylidene) benzohydrazide

K. Ananthi[1], S. Akshaya[2], H. Anandalakshmi[3]*
Research Scholar, Department of Chemistry, Annamalai University, India.[1,2]
Assistant Professor, Department of Chemistry, Annamalai University, India.[3]

ARTICLEINFO

Article history:
Received 28 July 2023
Accepted 31 July 2023
Available online 09 Aug 2023

Keywords:
Hydrazone,
NMR,
IR,
X-ray crystallography,
Hirshfeld surface analysis,
DFT,
Molecular docking,
Antimicrobial activity.
.

ABSTRACT

Hydrazone derivatives have drawn much attention because of their large pharmacological applications. In the present work, the compound (E)-3-methoxy-N'-(1-phenylethylidene) benzohydrazide (3-MAPHN), noted was synthesized, and its 3D structure was determined by X-ray crystallography. Structural characterization by X-ray crystallography was supported by Density Functional Theory (DFT) calculations. Intermolecular interactions in the crystal network were determined using Hirshfeld surface analyses. The optimized geometry analysis and HOMO-LUMO of the molecule were computed using the DFT-B3LYP method and 6-311++G (d,p) basis set. The compound has a Orthorhombic system and $Pca2_1$space group with the parameters of a = 8.1494(4) A˚, b = 10.5844(6) A˚,c = 16.3976(9) A˚, α = 90 °, β = 90 °, γ = 90 °.and Z = 4, V = 1414.40(13)˚A^3. It forms an S(6) ring motif with an intermolecular N-H/O and C-H/O hydrogen bonds. Hirshfeld surface analysis and 2D fingerprint plots signify meaningful interactions in crystal packing [H-H (49.8%), C-H (24%), O-H (16.4%), N-H (3.9%), C-N (3.0%), C-O (2.4%) and C-C (0.5%) contacts]. Atomic charges were predicted using the Mulliken population analysis. The molecular electrostatic potential (MEP) picture was drawn using the same level of theory to visualize the chemical reactivity and charge distribution on the molecule. Antimicrobial activity and docking studies of 3-MAPHN revealed that the molecule posses antibacterial and fungal activity and the ability of drug resistance, respectively.

1. Introduction

Hydrazones are an important multipurpose class of organic molecules that play a vital role in many fields of science [1-4]. They can be synthesized readily and inexpensively by condensation of aromatic or aliphatic acid hydrazides (R-C (=O)-NH-NH2). Hydrazones are identified by the presence of an azomethine group (or Schiff bases), which is among the essential groups in bioactive heterocycles due to its electrical conductivity and its biodegradable properties among others [5-9]. Other desirable characteristics of hydrazones include a tendency towards crystallinity and high stability. For many years, there has been considerable interest in this class of compounds on account of their biological and pharmacological activities, presenting impressive anti-cancer [10], antifungal, antibacterial, antimalarial [11], anti-trypanosomal [12], antitumor [13], anti-inflammatory, antiplatelet, analgesic [14], antidiabetic [9], antiviral [15] etc. Therefore, at present a variety of research activities regarding Schiff bases are in progress.

In an earlier study, we reported the synthesis and characterization of (E)-3-methoxy-N'-(4-fluorobenzylidene) benzohydrazide [16] using single crystal X-ray diffraction, FT-IR, NMR and spectra. In the present study, we discuss the synthesis and characterization of (E)-3-methoxy-N'-(1-phenylethylidene) benzohydrazide (3-MAPHN) using single crystal X-ray diffraction, FT-IR and NMR spectra. The structural properties of 3-MAPHN has been elucidated using single crystal X-ray crystallography through density functional theory (DFT). Further, the existence of charge transfer between HOMO-LUMO has been carried out using Frontier molecular orbitals. The work also involves the computational studies with Hirshfeld surface analysis. Antimicrobial activity and docking studies of 3-MAPHN were studied, respectively.

Materials and methods

Synthesis of (E)-3-methoxy-N'-(1-phenylethylidene) benzohydrazide (3-MAPHN)

3-methoxybenzohydrazide(0.302 g, 2 mmol) and Acetophenone (0.370 g, 2 mmol) were dissolved in methyl alcohol(25 ml) along with few drops of acetic acid to get clear solution. The reaction mixture was taken in a RB flask

and refluxed on water bath for about 3 h. The process of reaction was monitored by thin layer chromatography (TLC). After completion of reaction, the methyl alcohol was distilled off by vacuum distillation. The separated (E)-3-methoxy-N'-(1-phenylethylidene) benzohydrazide (3-MAPHN) was recrystallized from methanol. The yield was 80% and the melting point is 116 °C.(uncorrected M.P)

Investigation techniques Single crystal X ray crystallography

Bruker D8 Venture SC-XRD system is used for 3D structure determination from single crystal in the SAIF Laboratory, IIT (M), Tamilnadu, India.

Spectral Studies

IR spectra were recorded on an AVATAR 330 FT-IR spectrometer in KBr pellets. ^{1} H and ^{13} C NMR spectra were recorded on a Bruker Avance FT NMR spectrometer operating at 400.23 MHz for ^{1} H and 100.62 MHz for 13 C. The spectral parameters for ^{1} H NMR was as follows: spectral width 8223.6859 Hz; acquisition time 3.98 s; number of data points 16 K; digital resolution 0.3 Hz; number of scans 16. For 13 C NMR the spectral parameters were as follows; spectral width 25,000 Hz; acquisition time 1.31 s; number of data points 32 K; digital resolution 5 Hz and number of scans 80. NMR measurements were made using 5 mm tubes. Solutions for recording 1 H NMR and 13 C NMR spectra were prepared by dissolving about 10 mg and 50 mg of the compounds, respectively, in 0.5 mL DMSO–d 6 .

Computational methods

DFT calculations [17, 18] were made using B3LYP/6-311 ++ G method. The calculated frequencies of IR and NMR values confirm the stability of compound. DFT calculations for optimized structure of 3-MAPHN used to analysis the structural properties were calculated using Crystal Explorer 3.0 [19].

Molecular docking

In molecular docking the ligand for docking studies was prepared using LigPrep, Schrodinger. The ligand has been geometrically refined and assigned an appropriate protonation state. The strength minimization has been carried out using the aid of the OPLS 2005 pressure subject. The target protein enoyl acyl and carrier protein reductase (InhA) from Mycobacterium tuberculosis was downloaded from the Protein Data Bank (PDB id: 2NSD) and the active site was chosen. The grid was assigned by picking the ligand as the centre of the grid and then the grid box was generated by applying default parameters. The docking change has been finished using GLIDE, Schrodinger, GLIDE XP (extra precision) techniques.

Results and discussion Crystal structure

The recrystallized (E)-3-methoxy-N'-(1-phenylethylidene) benzohydrazide (3-MAPHN) was dissolved in distilled methanol and left for evaporation. The crystal was formed after four days. The supernatant liquid was decanted. The crystal suitable for X-ray analysis was obtained after washing with methanol. Since single crystal X-ray crystallography has been recorded for 3-MAPHN its characterization has been discussed in detail.[20]

The parameters of unit cell for 3-MAPHN are a = 8.1494(4) A˚, b = 10.5844(6) A˚,c = 16.3976(9) A˚, α = 90 °, β = 90 °, γ = 90 °.and Z = 4, V = 1414.40(13)˚A^3. An ORTEP view with atom labelling system of 3-MAPHN is shown in Fig. 1. X-ray diffraction data and its refinements of the compound listed in Table 1. Compound crystallized in the Orthorhombic crystal system, with $Pca2_1$ space group and was found to adopt an E -configuration about its –C = N – bond. In this compound, the hydrazone linkage plays an important role.

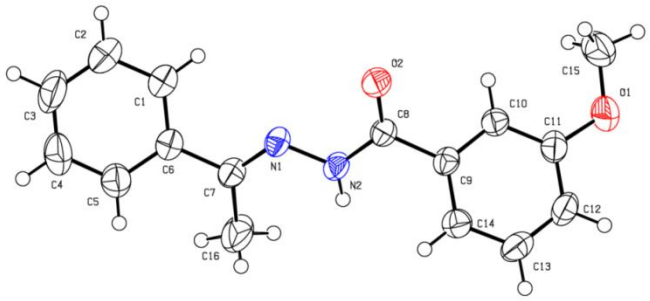

Fig. 1: ORTEP view with atom labelling system of 3-MAPHN

Table 1: Crystal data and structural refinement of 3-MAPHN

Identification code	**3-MAPHN**
Empirical formula	C16 H16 N2 O2
Formula weight	268.31
Temperature	296(2) K

Wavelength	0.71073 Å
Crystal system	Orthorhombic
Space group	$Pca2_1$
Unit cell dimensions	a = 8.1494(4) Å α= 90°. b = 10.5844(6) Å β= 90°. c = 16.3976(9) Å γ = 90°.
Volume	1414.40(13) $Å^3$
Z	4
Density (calculated)	1.260 Mg/m^3
Absorption coefficient	0.084 mm^{-1}
F(000)	568
Crystal size	0.300 x 0.250 x 0.200 mm^3
Theta range for data collection	3.850 to 26.740°.
Index ranges	-10<=h<=10, -13<=k<=13, -20<=l<=20
Reflections collected	33163
Independent reflections	2997 [R(int) = 0.0493]
Completeness to theta = 25.242°	99.2 %
Absorption correction	Semi-empirical from equivalents
Max. and min. transmission	0.7454 and 0.6339
Refinement method	Full-matrix least-squares on F^2
Data / restraints / parameters	2997 / 1 / 188
Goodness-of-fit on F^2	1.129
Final R indices [I>2sigma(I)]	R1 = 0.0390, wR2 = 0.0845
R indices (all data)	R1 = 0.0478, wR2 = 0.0903
Absolute structure parameter	0.0(5)
Extinction coefficient	0.107(10)
Largest diff. peak and hole	0.130 and -0.120 $e.Å^{-3}$
CCDC	2053078

The bond length of carbonyl C8=O2 and C7=N1 is observed as 1.220 A˚ and 1.278 A˚, respectively, which is exactly matches with the literature review[21, 22] . The selected bond lengths, bond angles, torsion angles of the title compound are listed in **Tables 3, 4 & 5**, which are Within the normal ranges[23] and comparable to those corresponding in other similar compounds[24]. The bond length of atoms C(8) and N(1) is similar to that observed in other Schiff bases[25-28], indicating it is a double bond. The bond length of C(7) and N(2), is intermediate between C–N and C=N bonds due to the conjugation effects in the molecule. The mean planes of the two benzene rings make a dihedral angle of 8.14(4)º. The methoxy benzylidene phenyl and phenylethyledene phenyl rings of 3-MAPHN were found to joined together through an open chain carbonyl hydrazone (–C =N –NH –CO –) system, in which all the atoms are in the same plane. Besides, both methoxybenzoyl phenyl and phenylethyleden phenyl rings of3-MAPHN are also lie in the same plane formed by –C =N – bond. The resulted that the bond lengths and bond angles are in good agreement with the standard values. As expected, the molecule adopts a trans configuration about the C=N double bond. The torsion angles C(6)-C(7)-N(1)-N(2), O(2)-C(8)-N(2)-N(1),C(7)-N(1)-N(2)-C(8) and C(9)–C(8)–N(2)–N(1) are 178.4(2), 0.3(4), –179.8(2) and 179.8(2), respectively. Three intramolecular hydrogen bonds are observed in the molecular structure. The lattice water and hydroxyl group of the Schiff base in the crystal are linked to the Schiff base moieties through intermolecular N–H···O and C-H···O hydrogen bonds (**Table 2, Fig.2**). The compound extends further to its final three-dimensional network through intermolecular N-H···O and C-H···O hydrogen bonds which interlink the molecules to stabilize the structure.

Table 2. Hydrogen bonds for 3-MAPHN [Å and °].

D-H...A	d(D-H)	d(H...A)	d(D...A)	<(DHA)
C(15)-H(15C)...O(1)#1	0.96	2.50	3.455(4)	174.8
C(16)-H(16A)...O(2)#2	0.96	2.40	3.066(4)	126.3
N(2)-H(2A)...O(2)#2	0.86(3)	2.27(3)	3.115(3)	170(3)

Symmetry transformations used to generate equivalent atoms:
#1 x+1/2,-y,z #2 x-1/2,-y+1,z

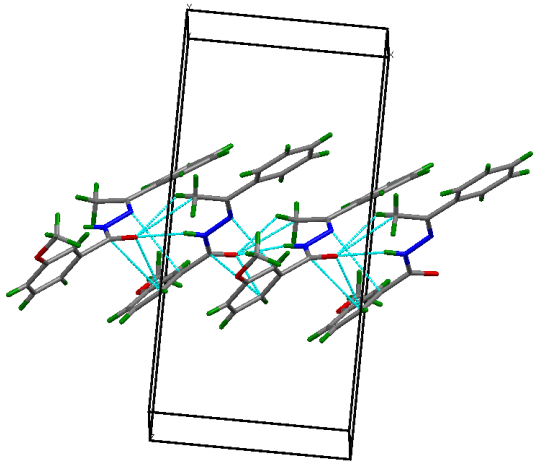

Fig. 2: Intermolecular hydrogen bonds in 3-MAPHN

Table 3: Bond lengths [Å] for 3-MAPHN

Atoms	Experimental	Theoretical	Atoms	Experimental	Theoretical
C(1)-C(6)	1.387(4)	1.421	C(11)-O(1)	1.369(3)	1.390
C(5)-C(6)	1.388(4)	1.408	N(1)-N(2)	1.379(3)	1.372
C(6)-C(7)	1.488(3)	1.484	N(2)-H(2A)	0.86(3)	1.013
C(7)-N(1)	1.278(3)	1.303	C(15)-O(1)	1.415(4)	1.452
C(7)-C(16)	1.486(4)	1.514	C(15)-H(15A)	0.9600	1.089
C(8)-O(2)	1.220(3)	1.243	C(13)-C(14)	1.394(4)	1.398
C(8)-N(2)	1.351(3)	1.391	C(16)-H(16A)	0.9600	1.096
C(8)-C(9)	1.497(3)	1.498			

Table 4: Bond angles [º] for 3-MAPHN

Atoms	Experimental	Theoretical	Atoms	Experimental	Theoretical
C(1)-C(6)-C(5)	118.0(2)	118.35.	C(10)-C(9)-C(8)	117.4(2)	117.957
C(1)-C(6)-C(7)	120.7(2)	119.647	C(11)-C(10)-C(9)	119.4(2)	120.141
C(5)-C(6)-C(7)	121.3(2)	121.997	C(11)-C(10)-H(10)	120.3	120.347
N(1)-C(7)-C(16)	124.7(2)	123.130	O(1)-C(11)-C(10)	124.9(2)	123.449
N(1)-C(7)-C(6)	116.2(2)	115.931	O(1)-C(11)-C(12)	114.9(2)	115.119
C(16)-C(7)-C(6)	119.1(2)	120.939	C(7)-N(1)-N(2)	119.0(2)	119.684
O(2)-C(8)-N(2)	123.5(2)	123.073	C(8)-N(2)-N(1)	117.6(2)	118.852
O(2)-C(8)-C(9)	121.0(2)	122.170	C(8)-N(2)-H(2A)	121.3(18)	120.135
N(2)-C(8)-C(9)	115.5(2)	114.738	N(1)-N(2)-H(2A)	120.7(18)	120.954
C(14)-C(9)-C(10)	120.7(2)	119.643	C(11)-O(1)-C(15)	118.2(2)	118.831
C(14)-C(9)-C(8)	122.0(2)	122.381			

Table 5: Torsion angles [°] for 3-MAPHN

Atoms	Experimental	Theoretical	Atoms	Experimental	Theoretical
C(6)-C(1)-C(2)-C(3)	-1.4(6)	0.268	N(2)-C(8)-C(9)-C(10)	137.1(2)	155.755
C(1)-C(2)-C(3)-C(4)	1.5(6)	0.152	C(14)-C(9)-C(10)-C(11)	2.3(4)	-1.035
C(4)-C(5)-C(6)-C(1)	0.1(4)	0.338	C(8)-C(9)-C(14)-C(13)	-179.1(2)	179.684
C(4)-C(5)-C(6)-C(7)	179.7(3)	179.499	C(12)-C(13)-C(14)-C(9)	-1.1(4)	-0.522
C(1)-C(6)-C(7)-N(1)	21.8(4)	11.397	C(16)-C(7)-N(1)-N(2)	-1.6(4)	-1.289
C(5)-C(6)-C(7)-N(1)	-157.8(2)	-167.153	C(6)-C(7)-N(1)-N(2)	178.4(2)	178.720
C(1)-C(6)-C(7)-C(16)	-158.1(4)	-168.593	O(2)-C(8)-N(2)-N(1)	0.3(4)	-6.716
C(5)-C(6)-C(7)-C(16)	22.2(4)	12.258	C(9)-C(8)-N(2)-N(1)	179.8(2)	174.850
O(2)-C(8)-C(9)-C(14)	135.0(3)	15.778	C(7)-N(1)-N(2)-C(8)	-179.8(2)	174.120
N(2)-C(8)-C(9)-C(14)	-44.6(3)	-22.671	C(10)-C(11)-O(1)-C(15)	2.7(4)	1.336
O(2)-C(8)-C(9)-C(10)	-43.3(4)	-25.795	C(12)-C(11)-O(1)-C(15)	-177.3(3)	178.256

Spectral analysis

FT-IR spectrum

IR spectra of 3-MAPHN were recorded and displayed in Plot 1. Generally, the carbonyl stretching vibration of ketones, aldehydes, carboxylic acids, amides and lactams [29] were absorbed in the region 1870-1540cm-1. Hence, in the IR spectrum (plot 1) of 3-MAPHN the absorption observed at 1654cm^{-1} and 1586 cm^{-1} were assigned to carbonyl (C=O) and nitrile (C=N) group, respectively. The presence absorption of carbonyl (C=O) and nitrile (C=N) group confirm the formation of hydrazones. The absorption bands observed at 3075 cm^{-1} and 3212cm^{-1} were assigned to C-H and N-H stretching frequencies of 3-MAPHN, respectively. The vibrational frequencies[30-32] of solid phase FT-IR spectrum of 3-MAPHN (Plot 1) and that obtained through a calculation using the B3LYP/6-311++G basis set were compared and tabulated in Table 6. Since the calculated and experimental vibrational wavenumbers of 3-MAPHN are almost matched with each other, it confirms the optimized structure (Fig. 3) of 3-MAPHN.

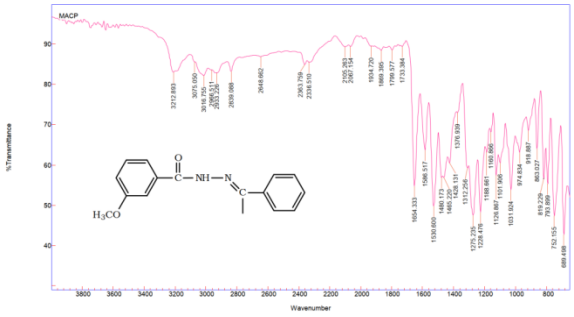

Plot 1: IR spectrum of 3-MAPHN

Table 6: Comparison of some selected experimental andcalculated vibrational wavenumbers (cm^{-1}) of 3-MAPHN at the B3LYP/6-311++G level of theory

Assignments	3-MAPHN	
	Experimental Values	Calculated values
C=O str.	1654	1655
C=N str.	1586	1588
C-N str.	1312	1318
N-N str.	1031	1034
N-H str.	3212	3217
N-H def.	1568	1570
C-H str.	3075	3082
C-H in plan (def.)	1442,1376	1448,1368
C-H out plan (def.)	974,918,863	868,922,974
C-CH3 str.	2933	2938
C-CH3 def.	689	688
C=C str.	1480	1480
OCH3 str.	2839	2842

^{1}H and ^{13}C NMR spectra

Assignments of [1] H NMR signals have been made using the position, integral values and coupling constants of the signals [33]. The [1] H NMR spectrum of 3-MAPHN is displayed in **Plot 2**, there is a signal at 3.83 ppm corresponding to three protons is due to the methoxy(OCH_3) protons of the compound.

Another signals at 10.76 ppm corresponds to NH proton. The signal at 2.50 ppm corresponding to two proton is due to the CH_3 proton of the compound. There are five signals in the range 6.94 to 7.86 ppm corresponding to eight protons are due to aromatic protons. From the observed frequencies of lines due to aromatic protons, the various proton coupling constants were determined.

Table 7: The experimental and calculated ^{1}H and ^{13}C chemical shift values of 3-MAPHN

Protons	3-MAPHN			
	^{1}H		^{13}C	
	Experimental Values	Calculated values	Experimental Values	Calculated values
CH_3	2.50	2.32	15.14	15.89
OCH_3	3.83	3.72	55.76	59.21
Aromatic	6.94-7.86	6.22-7.86	112.55-138.58	118.21-164.81
NH	10.76	9.87	-	-
C=O	-	-	159.59	141.54
C=N	-	-	166.11	176.05

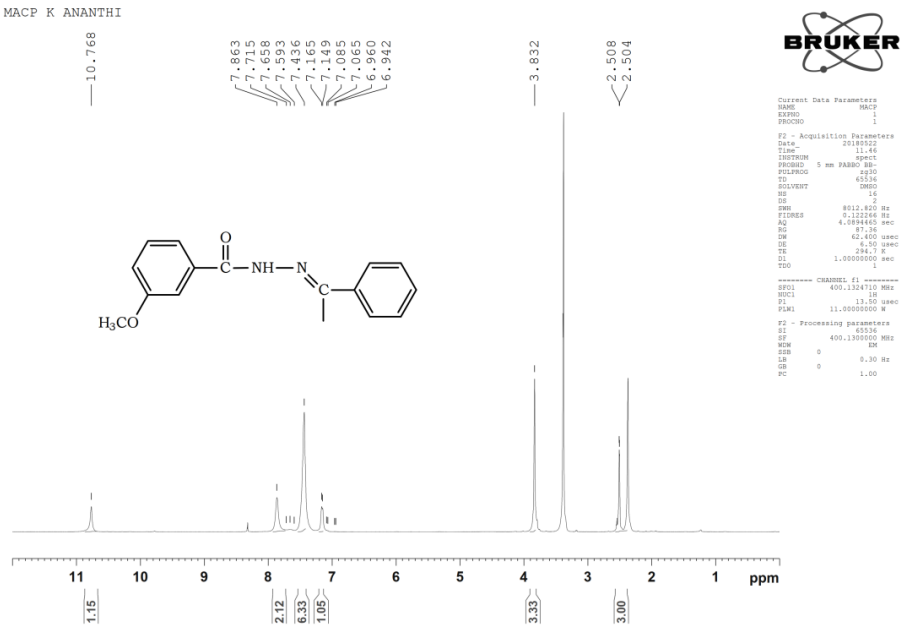

Plot 2: ^{1}H NMR spectrum of 3-MAPHN

The assignments of [13] C NMR signals have been made using the position and intensity of the signals. The [13] C NMR spectrum of 3-MAPHN is displayed in **Plot 3**, there is a signals at 166.11 ppm which is due to carbonyl carbon respectively. The signals at 159.59 ppm is assigned to azonitrile carbon (C =N). The signals obtained in the range of 112.55 to 138.58 ppm are due to aromatic carbons.

The theoretical and calculated 1H and 13C NMR chemical shift values were tabulated in Table 7. The assigned ^{1}H and 13C NMR signals are in accordance with the chemical shift values obtained through theoretical. Thus, the proposed structure of 3-MAPHN was confirmed through NMR assignment.

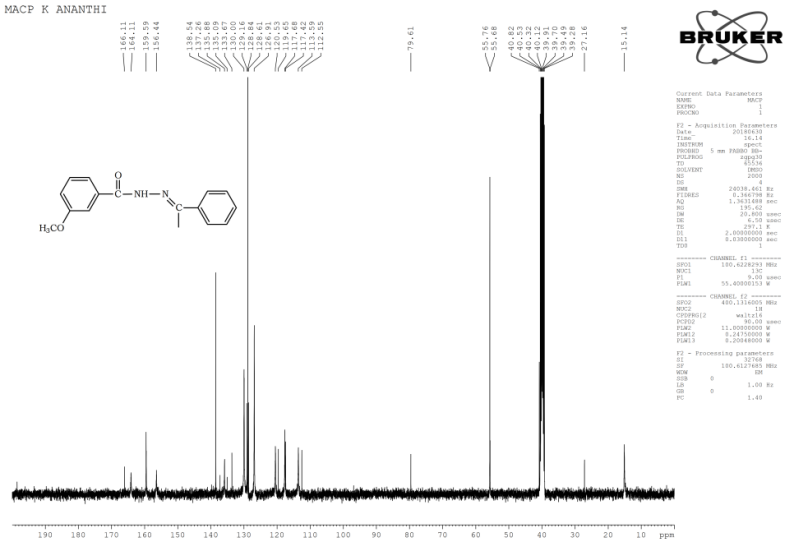

Plate 3: ^{13}C NMR spectrum of 3-MAPHN

DFT quantum chemical calculations for Optimized structure of 3-MAPHN

For the optimized structure of 3-MAPHN crystals shown in Fig. 3, DFT quantum chemical calculations have been carried out using the B3LYP/6-311++G basis set. The values of bond lengths, bond angles and torsion angles obtained by DFT calculation [21] were compared with the experimental values and tabulated in Tables 3-5, respectively. Since the calculated and theoretical values were in good agreement, it confirms the most stable optimized structures of 3-MAPHN.

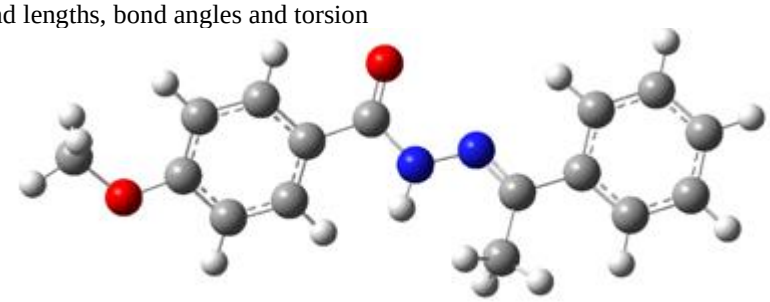

Fig. 3: Optimized structures of 3-MAPHN

Furthermore, the various bond lengths of both methoxy benzoyl phenyl and phenylethylidene phenyl rings of the optimized geometry are indicate that all the bond lengths of both the phenyl rings are almost equal and in good agreement between the calculated and experimental values. Moreover, analysis of various bond lengths apart from the phenyl rings the following observations were obtained. The bond lengths of C7-N1,C6-C7,C7-C16,N1-N2,C8-C9 , C15-O1and C11-O1 are 1.278Å, 1.488Å, 1.486Å, 1.379Å, 1.497Å, 1.415 Å & 1.369Å, respectively, they are in accordance with the theoretical values. Since the values range between 1.357-1.501 Å it indicates that the above bonds are single bonds in nature. Similarly, the bond lengths of C8-O2 and C8-N2 are 1.220 Å and 1.351 Å, respectively, they are in accordance with the theoretical values[34]. These bond length values indicate the double bond nature.

Analysis of bond angle values gives an idea about the orientation of phenyl rings. the bond angles of C14-C9-C8 (122.0°) and C5-C6-C7(121.3°) are greater than that of C10-C9-C8 (117.4°) and C1-C6-C7(120.7°). If both the phenyl rings are symmetry in nature all the bond angles should be around the normal angle of 120°.The observed increases and decreases of bond angles of the same phenyl rings indicate clearly that methoxy benzoyl phenyl ring slightly tilted towards the carbonyl group and the phenylethylidene phenyl ring. It was further supported by the greater value of observed bond angles about C8-N2-N1 (117.6°) than that obtained through an experimental value of 118.85°.

First-order hyperpolarizability

The first order hyperpolarizability (β0), dipole moment (μ) and polarizability (α0) of 3-MAPHN was calculated using B3LYP/6-311++G (d,p)shown in **Table 8**. The

mean polarizability α0 and total polarizability were -1.7X10^{-30}esu and 4.13X10^{30} esu. respectively. The total molecular dipole moment and first order hyperpolarizability of 3-MAPHN were 5.4102 Debye and 1.02X10^{-30} esu. Since the first order hyperpolarizability of3-MAPHN greater than that of urea (β=0.3728 X10-30esu), it confirms the nonlineority (NLO) characteristics and electronic properties of the compound.

Table 8: The Non-Linear measurements of 3-MAPHN

Parameters	**3-MAPHN** (B3LYP/6311++G(d,p)
Dipole moment (μ)	Debye
μ_x	-1.6060
μ_y	-3.7041
μ_z	3.6015
μ_{total}	5.4102
Polarizability (α0)	X10^{-30}esu
α_{xx}	-93.5166
α_{yy}	-134.456
α_{zz}	-107.454
α_{xy}	-6.7988
α_{xz}	-4.1842
α_{yz}	-2.9141
α_o *(esu)x10^{-23}*	***-1.7***
$\Delta\alpha$ *(esu) x10^{-24}*	***4.13***
Hyperpolarizability (β0)	X10^{-30}esu
β_{xxx}	-103.248
β_{yyy}	-43.2366
β_{zzz}	-0.4916
β_{xyy}	3.6722
β_{xxy}	-32.2668
β_{xxz}	11.9422
β_{xzz}	11.4977
β_{yzz}	1.7456
β_{yyz}	18.1744
β_{xyz}	19.4523
β_0 (esu) x10^{-30}	**1.02**

esu – electrostatic unit; Standard dipole moment (μ) for urea = 1.3732 Debye;
Hyperpolarizability (β0) for urea = 0.3728X10^{-30}esu.

Frontier molecular orbital

The conjugated molecules were characterized by a HOMO-LUMO separation, which will be the result of a significant degree of inter atomic charge transfer from the electron-contributor groups to the electron-acceptor groups through p-conjugated path[20]. The HOMO represents the capability to donate an electron;LUMO represents the capability to receive an electron. The energygap between HOMO and LUMO determines chemical reactivity, chemical hardnesse and softness of a molecule. The HOMO-1 and HOMOdenotes the second highest and highest occupied MOs and LUMO, LUMO+1 denotes the lowest and the second lowest unoccupied MOs respectively. The plots of HOMOs and LUMOs were shown in **Figs.4 a &b.**

The calculated energy values of the HOMO and LUMO of 3-MAPHN were-5.87792eV and -1.48975eV respectively by B3LYP level of calculations. Similarly, the HOMO-1 and LUMO+1 energy values is -6.29122eV and -0.66719eV by B3LYP level of calculations respectively. In this molecule, the energy gap between the HOMO LUMO/HOMO-1 LUMO+1 was 4.43604 eV and 3.54715eV, were the values are reproduced in **Fig. 4**

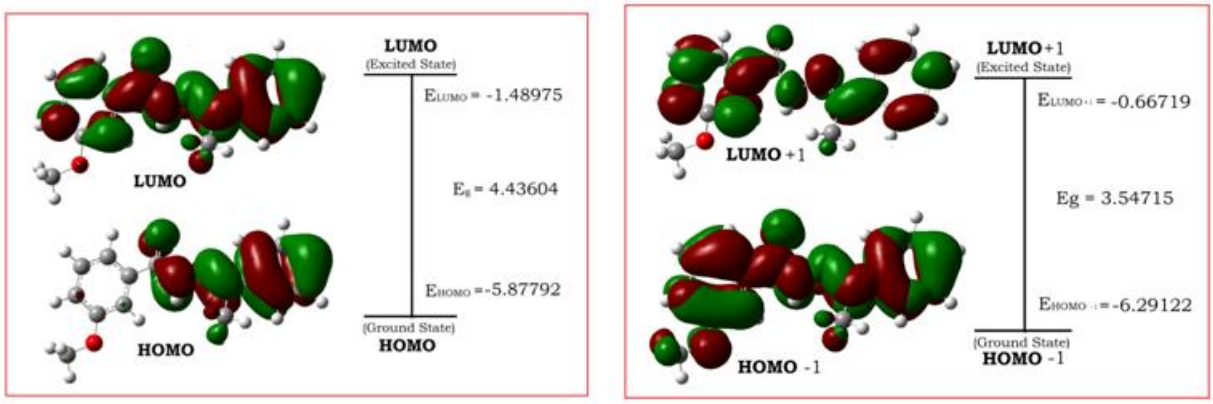

Fig. 4 (a & b). The frontier molecular orbitals of 3-MAPHN

. The chemical hardness and softness of a molecule was a sign of the chemical stability of a molecule. From the HOMO-LUMO energy gap, we can see that whether molecule was difficult (hard) or delicate (soft). If the molecule had large energy gap then the molecule can be called as hard molecule and the presence of small energy gap makes the molecules soft. The soft molecules were more polarizable than the hard ones because they need small energy for excitation.

The calculated values of the hardness, softness of our molecule were 2.1986 by B3LYP level of calculations as shown in **Table 9**. Therefore from the calculation we conclude that the molecule taken underneath investigation belongs to the hard materials.

Table 9: Calculated energy values of 3-MAPHN by B3LYP/6-31G++(d,p) level of calculation.

Energies	3-MAPHN B3LYP/6-31G++(d,p)
EHOMO (eV)	-5.87790
ELUMO (eV)	-1.48975
EHOMO-1 (eV)	-6.29122
ELUMO+1 (eV)	-0.66719
EHOMO - ELUMO gap (eV)	4.436049
EHOMO-1 – ELUMO+1 gap (eV)	3.53715
Chemical hardness (η)	2.21745
Softness (S)	0.2254
Chemical potential (μ)	-3.423
Electronegativity (χ)	-3.6206
Electrophilicity index (ω)	2.9558

Natural Population Analysis

The atomic charges greatly affect molecular system properties such as the dipole moment, the electronic structure, the acidity basicity behavior, and the vibration mode[20]. The atomic charges of the neutral, cationic and anionic species of 3-MAPHN were determined by natural population analysis (NPA) using B3LYP/6-31G++(d,p) method were the values are shown in **Table 10 Fig. 5**. For the compound 3-MAPHN among the methoxy benzelidene and phenylethylidene ring carbon atoms C1 (0.273e), C3 (0.023e) C16(0.502) C21(0.191e)and C22 (0.066e) of the molecule have positive charges. The positive charge on C1, C3, C16, C21, C22 is due to the attachment of nitrogen N18-N20 atoms to it respectively.

Also C1 (0.273e) and C16 (0.502e) have the highest positive charge this is due to the substitution of oxygen (O11,O17 atoms respectively. Hydrogen atoms of H8 (0.167e), H34 (0.158e), H35 (0.170e) and H36 (0.170e) have the highest positive charge when compare to the other hydrogen atoms; This is due to the binding to an atom with higher electronegativity, oxygen atoms (O11,O17) which could easily deprotonate in suitable medium.The oxygen atom O11 (-0.564) has the negative charge, reason for this high negative charge is (C-H...O) intermolecular hydrogen bonding. Similarly the nitrogen atom of N18 (-0.556 e) has the high negative charge due the presence of (N-H...O) intermolecular hydrogen bonding. The calculated atomic charge distribution was explained in the form of bar diagram shown in **Fig. 6** for 3-MAPHN.

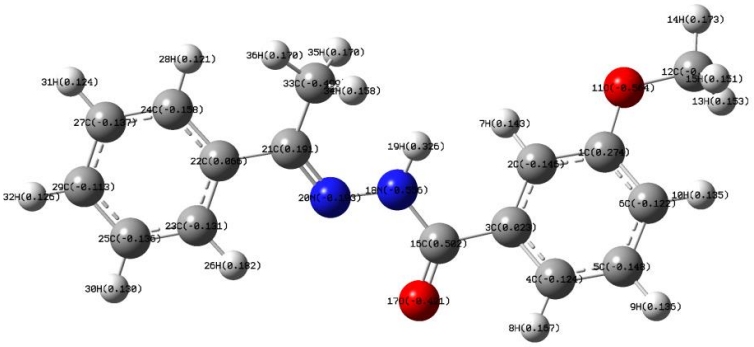

Fig.5: Mulliken atomic charge distribution of 3-MAPHN

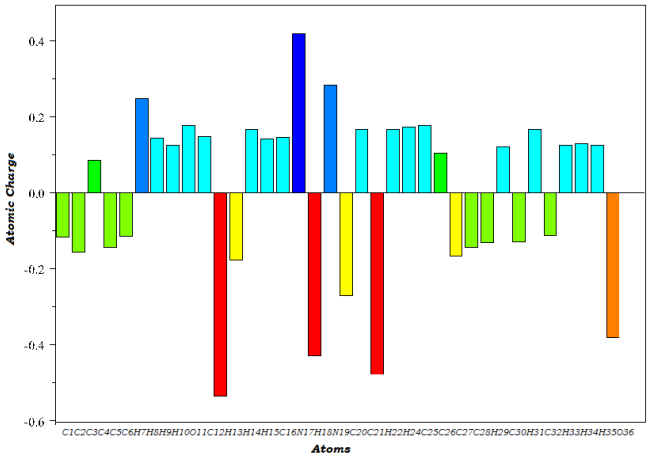

Fig. 6. Bar diagram of Mulliken atomic charges for 3-MAPHN

Table 10: Mulliken atomic charges for 3-MAPHN

Atoms	Atomic Charges (a.u)	Atoms	Atomic Charges (a.u)	Atoms
C1	0.274	H13	0.153	H26
C2	-0.146	H14	0.173	C27
C3	0.023	H15	0.151	H28
C4	-0.124	C16	0.502	C29
C5	-0.148	O17	-0.421	H30
C6	-0.122	N18	-0.556	H31
H7	0.143	H19	0.326	H32
H8	0.167	N20	-0.193	C33
H9	0.136	C21	0.191	H34
H10	0.135	C22	0.066	H35
O11	0.564	C23	-0.131	H36
C12	-0.172	C24	-0.158	H26

Molecular electrostatic potential

The molecular electrostatic potential (MEP) is the plot of electrostatic potential mapped on to the constant electron density surface, allowing the prediction of sites and relative reactivity towards electrophilic attack and nucleophilic reactions of molecules. The MEP is widely used as a reactivity map displaying most probable regions for the electrophilic attack of charged point like reagents on organic molecules. MEP plot provides a simple way in predicting the interaction of different geometries. In order to predict the reactive sites for electrophilic and nucleophilic attacks of the 3-MAPHN , MEP was calculated with B3LYP/6-311++G(d,p) basis set optimized geometry is computed[20, 35, 36]. The negative (red color) and positive (blue color) regions of MEP are

related to electrophilic and nucleophilic reactivity, respectively shown in **Fig. 7 (a)**. The negative region is located over the O11 atoms the positive region is located over H19 atom of 3-MAPHN in the hydrazone linkage.

The red and blue colored regions indicate the negative electrostatic potential (nucleophiles) and positive electrostatic potential (electrophile), respectively. The green region shows neutral potential. The MEP map of 3-MAPHN is in the range of -7.975×10^{-2} V to 7.975×10^{-2} V, respectively. For the compound 3-MAPHN, the total electron density surface mapped with electrostatic potential indicates the presence of a high negative charge on the oxygen O11 atom of the carbonyl group. Although, the positive region of the MEP map is localized over the N-H group, indicating that they are susceptible sites for nucleophilic attack. Analyses of the MEP surface of these compounds represent the availability of electrons for possible interaction with another group of atoms. The MEP results are supported by the electrostatic potential contour map showing the lines isosurface in **Fig. 7 (b)**.

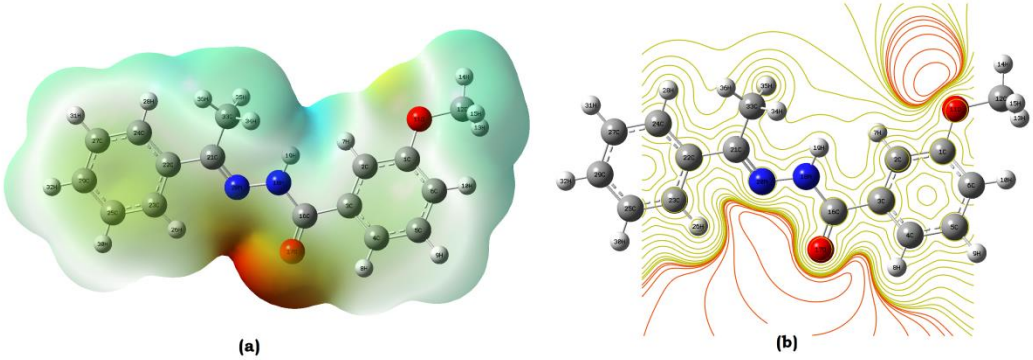

Fig.7 a & b. The molecular electrostatic potential of 3-MAPHN

Hirshfeld Surface analysis

The nature of the intermolecular contacts[37, 38] and their quantitative contributions to the crystal packing for the compound were analysed by Hirshfeld surface analysis and two-dimensional fingerprint plots, generated using CrystalExplorer3.1.[39]. For the calculations, the experimental atom positions in the CIF file were used. The Hirshfeld surfaces of the two compounds were mapped with different properties, namely, dnorm, di and de shown in **Fig.8** . The views of the surface were obtained in the range 0.3871 to 1.3554 (dnorm),0.7196 to 2.8395 (di), and 0.92903 to 2.5235 a.u (de). On the Hirsh feld surface mapped with dnorm, there are three colours; red, blue, and white. Red spots on the Hirshfeld surface are related to hydrogen bonding N-H···O interactions between the corresponding donor and acceptor atoms are visualized. The contacts near the vander Waals separation are indicated with the white spots, and longer contacts are shown with the blue spots. The presence of other light red spots in 3-MAPHN correspond to the C-H···O interactions, which are considered to be weak interactions. The 2D fingerprint plots, which are used to analyse all of the intermolecular contacts at the same time, revealed that the main intermolecular interactions in the compound were H...H, O...H and C...H shown in **Fig. 9**.

For 3-MAPHN the contributions of the intercontacts to the Hirshfeld surface are H-H (49.8%), C-H/H-C (24.0%) and O-H/H-O (16.4%); the results of the Hirshfeld surface analysis are shown in **Fig. 9** (i-viii). Besides,the O-H/H-O contacts display the existence of intermolecular N-H..O and C-H...O interactions. Also, there are other small percentage contribution to Hirshfeld surface from the different interatomic contacts: NNH/H-N (3.9%), N-C/C-N (3.0%), C-C (2.4%) and C-O (0.5%). These interactions indicate the formation of intermolecular hydrogen bonding

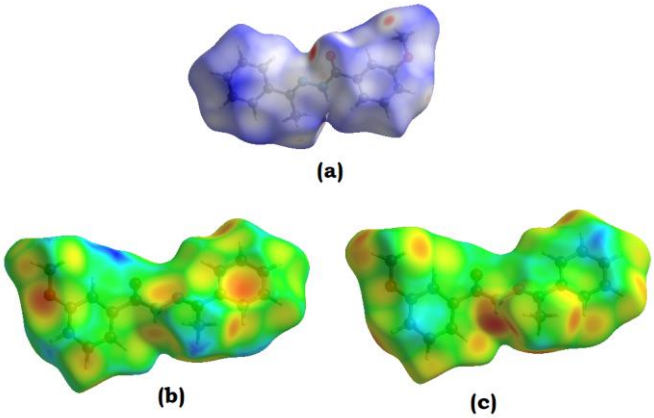

Fig.8. Inter contacts within the crystal of 3-MAPHN. (a) dnorm (b) de (c) di

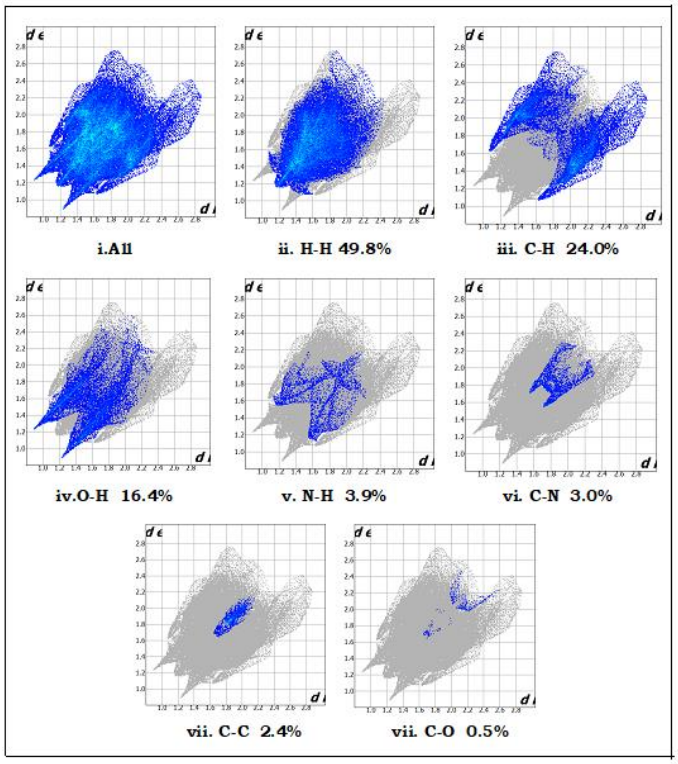

Fig. 9: 2D Fingerprint plots of 3-MAPHN (i) full; showing reciprocal contacts and resolved into: (ii) H...H, (iii) C...H, (iv) O...H, (v) N...H, (vi) C...N and (vii) C...C (viii) C…O showing the percentage contact contributing to the total Hirshfeld surface of the molecule. Black arrows are show spike for different interactions.

Molecular docking

To find a suitable inhibitor for Mycobacterium tuberculosis docking studies[40-41] was carried out for InhA protein. In the biosynthesis of Mycobacterium Tuberculosis[42], InhA catalyzes the reduction of lengthy chain trans-2-enoyl-ACP present inside the fatty acid. Inhibition of InhA disrupts the biosynthesis of the mycolic acids that had been valuable components of the mycobacterial cellular wall. Results of the docking studies revealed that the ligand 3-MAPHN shows a high glide score and interaction energy was shown in Table 11. These compound showes a interaction with TYR 158. Therefore based on the docking studies, the compound 3-MAPHN is possibly appropriate to beat the drug resistance of Mycobacterium tuberculosis InhA protein. The docking interaction of compound were shown in Fig.10 (a&b).

Table 11: Molecular docking results of 3-MAPHN with 2NSD

Compound	Glide gscore	Glide energy	Glide evdw	Glide ecoul	Interacting Residues
3-MAPHN	-9.072	-51.151	-44.807	-6.344	H-Bond interaction with TYR 158
Standard (isoniazid)	-13.042	-57.000	-50.841	-6.158	LYS165, PHE149, H-Bond interaction with HOH
glide evdw = van der Waals interaction energies, glide ecoul = Coulomb interaction energies					

Antimicrobial activity

Antibacterial activity [43] of the synthesized compound 3-MAPHN was carried out using standard disk diffusion method. For this study Ciprofloxacin has been used as standard. The sample and the standard solutions were prepared by dissolving 200 µg/ mL in DMSO. Nutrient agar medium was inoculated with different microorganisms and once the media was solidified, it was punched with a 6 mm diameter well. To the agar plates

containing bacteria the sample and the standard solutions were added and incubated at 37 °C for 24 h. Then the antibacterial activity of the sample solution was analysed by compared with the standard solution.

In this study, the compound 3-MAPHN was screened against two gram positive bacterial strains viz., Staphylococcus aureus, Streptococcus pyogens and two gram negative bacterial strains viz., Escherichia coli and Pseudomonas aeruginosa along with Ciprofloxacin as standard .The antibacterial activity of the sample solution was compared with the standard solution and the values are shown in Table 12. The analyses shows that the compound exhibits a reasonable activity in opposition to the Streptococcus aureus and Escherichia coli bacteria compare to others. Hence, it is concluded that the compound 3-MAPHN is having moderate antibacterial activity.

The compounds 3-MAPHN were examined for their antifungal activity against strains: candida albicans, cryptococcus neoformans and aspergillus nigar using Amphotericin B as standard through disc diffusion approach. The MIC values are given in Table 12. The compounds exhibit moderate antifungal activity against tested fungal strains.

Table 12: Antimicobial activities of 4-APEBH.results of 3-MAPHN with 2NSD

Zone of inhibition in diameter (mm)							
Compounds	Gram positive		Gram negative		Fungus		
	Staphylococcus aureus	*Streptococcus pyogens*	*Escherichia coli*	*Pseudomonas aeruginosa*	*Candida albicans*	*Cryptococcus neoformans*	*Aspergillus niger*
3-MAPHN	9	15	9	10	9	10	11
Control	39	32	11	40	18	18	10

Conclusion

The synthesis of new benzohydrazide derivative (E)-3-methoxy-N'-(1-phenylethylidene) benzohydrazide (3-MAPHN) by simple and convenient methodology. The structural characterization and IR, NMR analysis were also discussed. X-ray crystallographic studies for 3-MAPHN display intermolecular N-H...O, and C-H...O hydrogen bonding and C-H π interactions, forming layers in the crystal lattice. The results of Hirshfeld surface analysis indicate that the major interactions were found for H-H interaction with contribution of 49.8% of the total Hirshfeld Surface area in the product, respectively. Frontier molecular orbital analysis and molecular electrostatic potential maps of compound have been studied using DFT calculations. The molecular electrostatic potential analysis gives information about intermolecular interaction regions. The results indicate that compound 3-MAPHN with a smaller LUMO-HOMO gap, more reactive.The molecular electrostatic potential of the studied compounds showed suitable regions to attack for nucleophilic and nucleophilic substances. The result of antibacterial and antifungal activities of compounds 3-MAPHN showed that moderately active against the tested bacterial and fungal strains. Antimicrobial activity and docking studies of 3-MAPHN revealed that the molecule posses antibacterial activity and the ability of drug resistance, respectively.

Refferences

1. A. Kajal, S. Bala, N. Sharma, S. Kamboj, V. Saini, Therapeutic potential ofhydrazones as anti-in ammatory agents, Int. J. Med. Chem. (2014), https://doi.org/10.1155/2014/761030 .

2. J. Galeta, S. Man, M. Potacek, Substituted homoallenyl aldehydes and their derivatives. Part 1: homoallenyl aldehydes and protected hydrazones, Chem.Pap. 67 (2013) 29e39, https://doi.org/10.2478/s11696-012-0215-6 .

3. C. Gokce, R. Gup, Synthesis and characterisation of Cu(II), Ni(II), and Zn(II)complexes of furfural derived from aroylhydrazones bearing aliphatic groupsand their interactions with DNA, Chem. Pap. 67 (2013) 1293 e1303, https://doi.org/10.2478/s11696-013-0379-8 .

4. J. Wu, D.-D. Xie, W.-L. Shan, Y.-H. Zhao, W. Zhang, B. Song, S. Yang, J. Ma,Synthesis and insecticidal activity of anthranilic diamides with hydrazonesubstructure, Chem. Pap. 69 (2015) 993 e1003, https://doi.org/10.1515/chempap-2015-0100 .

5. S. Rollas, S.G. Küçükgüzel, Biological activities of hydrazone derivatives,Molecules 12 (2007) 1910 e1939.

6. N. Noshiranzadeh, A. Heidari, F. Haghi, R. Bikas, T. Lis, Chiral lactic hydrazone derivatives as potential bioactive antibacterial agents: synthesis, spectroscopic, structural and molecular docking studies, J. Mol. Struct. 1128 (2017)391-399.

7. C. Fattorusso, G. Campiani, G. Kukreja, M. Persico, S. Butini, M.P. Romano, M. Altarelli, S. Ros, M. Brindisi, L. Savini, Design, synthesis, and structure eactivity relationship studies of 4-quinolinyl-and 9-acrydinylhydrazones as potent antimalarial agents, J. Med. Chem. 51 (2008)1333-1343.

8. G. Verma, A. Marella, M. Shaquiquzzaman, M. Akhtar, M.R. Ali, M.M. Alam,A review exploring biological activities of hydrazones, J. Pharm. BioAllied Sci.6 (2014) 69 .

9. S. Rollas, S. Küçükgüzel, Biological activities of hydrazone derivatives, Mole-cules 12 (2007) 1910 -1939.
10. Z. Cui, Y. Li, Y. Ling, J. Huang, J. Cui, R. Wang, X. Yang, New class of potentantitumor acylhydrazone derivatives containing furan, Eur. J. Med. Chem. 45(2010) 5576-5584.
11. C. Fattorusso, G. Campiani, G. Kukreja, M. Persico, S. Butini, M.P. Romano,M. Altarelli, S. Ros, M. Brindisi, L. Savini, Design, synthesis, and structure eactivity relationship studies of 4-quinolinyl-and 9-acrydinylhydrazones as potent antimalarial agents, J. Med. Chem. 51 (2008)1333-1343.
12. R. Narang, B. Narasimhan, S. Sharma, A review on biological activities and chemical synthesis of hydrazide derivatives, Curr. Med. Chem. 19 (2012) 569-612.
13. M.T. Cocco, C. Congiu, V. Lilliu, V. Onnis, Synthesis and in vitro antitumoralactivity of new hydrazinopyrimidine-5-carbonitrile derivatives, Bioorg. Med.Chem. 14 (2006) 366-372.
14. A.R. Todeschini, A.L.P. de Miranda, K.C.M. da Silva, S.C. Parrini, E.J. Barreiro,Synthesis and evaluation of analgesic, antiin ammatory and antiplateletproperties of new 2-pyridylarylhydrazone derivatives, Eur. J. Med. Chem. 33(1998) 189-199.
15. M.T. Abdel-Aal, W.A. El-Sayed, E.H. El-Ashry, Synthesis and antiviral evaluation of some sugar arylglycinoylhydrazones and their oxadiazoline derivatives, Arch. Pharm. Int. J. Pharm. Med. Chem. 339 (2006) 656-663.
16. K. Ananthi, H. Anandalakshmi, S. Senthilkumar,Spectral characterization and crystal structure of (E)-3-methoxy-N'-(4-fluorobenzylidene) benzohydrazide, Journal of Natural Remedies Vol. 21, No. 8(1), (2020)
17. A.D. Becke , Densityfunctional thermochemistry. III. The role of exact exchange, J. Chem. Phys. 98 (1993) 5648–5652 .
18. C. Lee , W. Yang , R.G. Parr , Development of the Colle-Salvetti correlation-energy formula into a functional of the electron density, Phys. Rev. B 37 (1988) 785-789 .
19. M.A. Spackman , J.J. McKinnon , Fingerprinting intermolecular interactions in molecular crystals, Cryst. Eng. Comm. 4 (66) (2002) 378-392 .
20. M.S. Alam, D.-U. Lee. Spec. chim. Acta A., 2015, 145, 563–574.
21. N. Ramesh Babu , S. Subashchandrabose , M. Syedalipadusha , H. Saleem , V. Manivannan , Y. Erdogdu , J. Mol. Struct. 1072 (2014) 84–93 .
22. N. RameshBabu , S. Subashchandrabose , M. Syedalipadusha , H. Saleem , Ind. J.
Appl. Res. 4 (2014) 1–6 .
23 .Allen, F. H.; Kennard, O.; Watson, D. G.; Brammer, L.; Orpen, A. G.; Taylor, R. Tables of bond lengths detemined by X-ray and neutron diffraction. Part1. Bond lengths in organic compounds. Chem. Soc., Perkin Trans. 1987, 2, S1–19.
24. Deng, S.; Han, L.; Huang, S.; Zhang, H.; Diao, Y.; Liu, K. (E)-N'-(5-Chloro-2-hydroxybenzylidene)-3,5-dihydroxybenzohydrazide monohydrate. Acta Cryst. 2009, E65, o721.
25. Li, J. M.; Li, J. Z.; Zhang, H. Q.; Li, J.; Zhang, Y. Synthesis and crystal structure of N,N'-Bis-[(1-phenyl-3-methyl-5-oxo-4-pyrazolinyl)-α-furylmethylidyne]ethylenediimine. Chin. J. Struc. Chem. 2010, 29, 1552.
26. Zhang, H. Q.; Li, J. Z.; Zhang, Y.; Zhang, D.; Su, Z. H. 4-[(Z)-(n-Butylamino)(2-furyl)methylene]-3-methyl-1-phenyl-1H-pyrazol-5(4H)-one. Acta
Cryst. 2007, E63, o3536.
27. Li, J.; Li, J. Z.; Li, J. Q.; Zhang, H. Q.; Li, J. M. 4-[(Z)-(2-Furyl)(2-naphthylamino)methylene]-3-methyl-1-phenyl-1H-pyrazol-5(4H)-one. Acta Cryst. 2009, E65, 1824.
28. Yuan. L.; Nan, Y.; Li, J. Y.; Huang, X. L. (E)-N'-(2-chlorobenzylidene)-3,5- dihydroxybenzohydrazide dihydrate. Acta Cryst. 2011, E67, o3017.
29. S. Sylvestre and K. Pandiarajan. Spec. chim. Acta A., 2011, 78, 153.
30. D.L. Vein, N.B. Colthup, W.G. Fateley, J.G. Grasselli, The Handbook of Infrared and Raman Characteristic Frequencies of Organic Molecules, 1st Edition, Academic Press, San Diego 1991 .
31. M. Silverstein, G.C. Basseler, C. Morill. Spectrometric identification of organic compounds, John Wiley & Sons, New York. 1981 .
32. X. Du, C. Guo, E. Hansell, P.S. Doyle, C.R. Caffrey, T.P. Holler, J.H. Mukerrow, F.E. Cohen. J. Mol. Chem., 2002 , 2695–2707.
33. G. Muthukumaran , J. Chakkaravarthy , K. Pandiarajan , S. Senthilkumar , J. Mol.
Struct. 1197 (2019) 262–270.
34. N. RameshBabu, S. Subashchandrabose, M. Syedalipadusha, H. Saleem. Ind. J. Appl. Res., 2014, 4, 1-6.
35. B. Kosar, C. Albayrak. Spectrochim. Acta A., 2011, 78, 160–167.
36. A.M. Kcoster, M. Leboeuf, D.R. Salahub, S.M. Jane, S. Kalidas. Theor. Compu. Chem. Els., 1996, 105–142.
37. M. A. Spackman, D. Jayatilaka. Cryst. Engg. Comm., 2009, 11, 19–32.
38. J.J. McKinnon, A.S. Mitchell, M.A. Spackman. Chem. Eur. J, 1998, 4, 2136–2141.
39. M. A. Spackman, J. J. McKinnon. Cryst. Eng. Comm., 2002, 4, 378–392.
40. I.B. Ramis, Tuberculosis., 2019, 118, 101-853.
41. G. F. Zha. Bioorg. Med. Chem. Lett., 2017, 27, 3148–3155.
42. U.B. Karale. Euro. J. Med. Chem., 2019, 178, 315-328.
43. I.B. Ramis , et al. , In silico and in vitro evaluation of tetrahydropyridine compounds asefflux inhibitors in Mycobacterium abscessus, Tuberculosis 118 (2019) 101853 .